Inorganic Chemistry

ARTICLE

pubs.acs.org/IC

# Iron(III) Chemistry with Ferrocene-1,1′-dicarboxylic Acid ($fdcH_2$): An $Fe_7$ Cluster with an Oxidized $fdc^-$ Ligand

Antonio Masello,[†] Yiannis Sanakis,[‡] Athanassios K. Boudalis,[‡] Khalil A. Abboud,[†] and George Christou*[,†]

[†]Department of Chemistry, University of Florida, Gainesville, Florida 32611-7200, United States

[‡]Institute of Materials Science, NCSR "Demokritos", 15310 Aghia Paraskevi Attikis, Greece

Supporting Information

**ABSTRACT:** The synthesis and properties are reported of a new $Fe_7$ cluster obtained from the reaction of ferrocene-1,1′-dicarboxylic acid ($fdcH_2$) with $FeCl_2 \cdot 4H_2O$ in MeOH under ambient light conditions. The compound is the mixed-anion salt $[Fe_7O_3(OMe)(fdc)_6(MeOH)_3][FeCl_4]Cl_2$ (**1**; $8Fe^{III}$), containing six ($fdc^{n-}$) groups as peripheral ligands. The cation of **1** has virtual $C_3$ symmetry and contains a central $[Fe_4(\mu_3\text{-}O)_3(\mu_3\text{-}OMe)]^{5+}$ cubane unit whose three oxide ions each become $\mu_4$ by attaching to a fourth Fe atom outside the cubane. The resulting $[Fe_7(\mu_3\text{-}O_3)(\mu_3\text{-}OMe)]^{14+}$ core is surrounded by six $fdc^{n-}$ ($n = 1, 2$) groups, which divide into two sets by virtual symmetry. The blue color of the complex suggested that some of these ligands are in their oxidized $fdc^-$ ferricenium ($Fe^{III}$) state, and various data point to there being one $fdc^-$ ligand in the compound, the initial example of the group acting as a ligand in inorganic chemistry. Variable-temperature, solid-state DC and AC susceptibility measurements reveal the cation to be antiferromagnetically coupled, as expected for high-spin $Fe^{III}$, and to have an $S = 2$ ground state, consistent with an $S = {}^5/_2$ $Fe_7$ inner core coupled antiferromagnetically to the one paramagnetic $fdc^-$ ($S = {}^1/_2$) ligand. Complex **1** displays multiple reductions and oxidations when investigated by electrochemistry in MeCN. $^{57}$Fe Mössbauer spectroscopy supports the presence of only five $fdc^{2-}$ ligands, but cannot resolve the signals from the various $Fe^{III}$ sites.

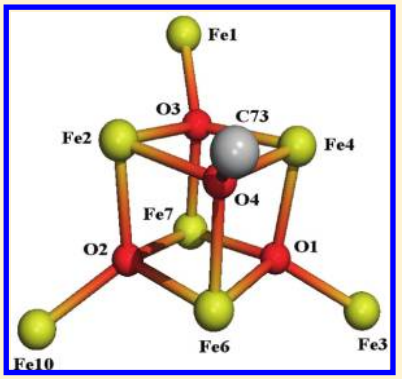


## INTRODUCTION

Molecular transition metal cluster chemistry continues to be of great interest to many research fields. Within the magnetism community, much of this interest has stemmed from the observation that such clusters provide a rich source of new molecules with high ground-state spin ($S$) values. When combined with a large Ising-like magnetoanisotropy (large and negative axial zero-field splitting parameter, $D$), such species function as single-molecule magnets (SMMs).[1] SMMs have a significant energy barrier to magnetization relaxation, and at temperatures below their blocking temperature ($T_B$) will function as nanoscale magnetic particles displaying magnetization hysteresis in the absence of intermolecular interactions and long-range ordering.

The large majority of our own work in high spin clusters and SMMs has concentrated on 3d metal oxo chemistry with either just carboxylate ligation or a mixture of carboxylates and other ligand types, such as azides in higher oxidation state ($Mn^{III}$, $Mn^{IV}$) chemistry.[2] Thus, when we recently decided to extend our efforts by incorporating redox-active ligands into our 3d cluster chemistry, we decided to base this on carboxylate ligation and chose to use ferrocene-1,1′-dicarboxylic acid ($fdcH_2$). In fact, the $fdc^{2-}$ anion is a very interesting dicarboxylate in that it (i) can undergo reversible one-electron redox chemistry, (ii) it is a dicarboxylate that can act as chelate and/or bridging ligand with restricted flexibility, and (iii) it can, however, rotate its cyclopentadienyl rings and bridge separate units to yield oligomeric or polymeric products. All these modes have been seen in the past for $fdc^{2-}$, which has been used with transition metals,[3,4] lanthanides,[5] and main group metals,[6] encompassing both coordination and organometallic chemistry. In fact, the bridging modes are common, and as a result $fdc^{2-}$ is often used in combination with other ligands to prevent polymeric products. In our own work to date, we have targeted metal-oxo products with only $fdc^{2-}$ ligands (other than bridging or terminal ligands derived from solvent molecules).

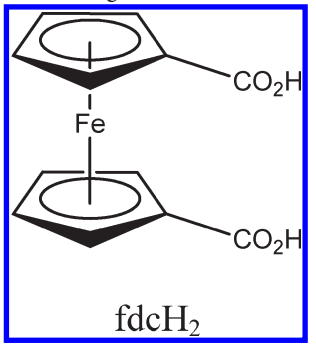


In our previously explored Mn chemistry with $fdc^{2-}$, we found this ligand to give molecular species, and had obtained three products, $[Mn_7O_3(OMe)(fdc)_6(H_2O)_3]$, $[Mn_8O_4(fdc)_6$

**Received:** February 18, 2011
**Published:** May 16, 2011

  

$(DMF)_2(H_2O)_2]$, and $[Mn_{13}O_8(OEt)_6(fdc)_6]$,[7] the last of which was a known complex but made by a different procedure.[3c] We have since extended this work to $Fe^{III}$, for which there were no known $fdc^{2-}$ compounds, although two compounds have since been reported.[3g] However, since these involve the binding of a single $fdc^{2-}$ onto $Fe^{III}_4$ and $Fe^{III}_6$ carboxylate starting materials, it is not pertinent to the goal of the present work, which is to obtain an $Fe^{III}$ oxo cluster with only $fdc^{2-}$ peripheral ligation. We herein report the synthesis, structure, electrochemical, and Mössbauer spectra of the first such cluster, the cation $[Fe_7O_3(OMe)(fdc)_6(MeOH)_3]^{3+}$.

## EXPERIMENTAL SECTION

**Syntheses.** All preparations were performed under aerobic conditions and at ambient conditions of temperature and light. All commercial chemicals were used as received.

**$[Fe_7O_3(OMe)(fdc)_6(MeOH)_3][FeCl_4]Cl_2$ (1).** To a stirred suspension of $fdcH_2$ (0.15 g, 0.50 mmol) in MeOH (25 mL) was added solid $FeCl_2 \cdot 4H_2O$ (0.20 g, 1.0 mmol). The mixture was stirred overnight with the room lights on, and then filtered to remove undissolved starting materials and byproducts. The filtrate was treated by slow diffusion with a mixture $Et_2O$/Hexane (1:1 v/v) and left exposed to the room light. X-ray quality blue crystals of **1**·*x*(solv) began to form after 2 days. When crystallization was judged complete after several more days, the crystals were separated from the mother liquor with a Pasteur pipet, washed with a minimal amount of $Et_2O$ and then with hexanes, and dried very briefly under vacuum. The yield of crystalline product was very low (15 mg, 5%). Anal. Calcd (Found) for **1**·$8H_2O \cdot 6$MeOH ($C_{82}H_{103}Fe_{14}O_{45}Cl_6$): C, 35.13 (35.01); H, 3.70 (3.29); N, 0.00 (0.02); Cl 7.59 (7.65) %. Selected IR data (KBr pellet, $cm^{-1}$): 1575 (vs), 1481 (vs), 1400 (vs), 1362 (s), 1195 (w), 1115 (w), 1082 (w), 1031 (vw), 928 (vw), 832 (vw), 781 (w), 621 (w), 589 (w), 522 (m), 491(m).

**X-ray Crystallography.** A suitable blue crystal of **1**·*x*(solv) was attached to a glass fiber using silicone grease and transferred to a goniostat where it was cooled to 173 K for data collection. Data were collected on a Siemens SMART PLATFORM with a CCD area detector and a graphite monochromator using $MoK_\alpha$ radiation ($\lambda$ = 0.71073 Å). Cell parameters were refined using 8192 reflections. A full sphere of data (1850 frames) was collected using the $\omega$-scan method (0.3° frame width). The first 50 frames were remeasured at the end of data collection to monitor instrument and crystal stability (maximum correction on *I* was <1%). Absorption corrections by integration were applied based on measured indexed crystal faces.

The structure was solved by direct methods in SHELXTL6,[8] and refined on $F^2$ using full-matrix least-squares cycles. The non-H atoms were treated anisotropically, whereas the H atoms were placed in calculated, ideal positions and refined as riding on their respective carbon atoms. The asymmetric unit consists of a $Fe_{13}$ cation, an $FeCl_4^-$ anion, and electron density assignable to the $Cl^-$ anions, and a large number of solvent molecules. The latter two are too disordered to be modeled; thus program SQUEEZE,[9] a part of the PLATON[10] software package, was used to calculate the disorder area and remove its contribution to the overall intensity data. In addition, three of the four Cl atoms of the $FeCl_4^-$ anion are disordered and were refined in two parts with site occupation factors of 0.577(2) and 0.423(2). A total of 1119 parameters were refined in the final least-squares cycles using 8375 reflections with $I > 2\sigma(I)$ to yield $R_1$ and $wR_2$ of 4.06 and 8.31%, respectively. Unit cell data and structure refinement details are collected in Table 1.

**Other Studies.** Infrared spectra were recorded on KBr pellets on a Nicolet Nexus 670 FTIR spectrometer in the 400−4000 $cm^{-1}$ range. Visible spectra were recorded in MeOH solution on a Jasco UV/vis spectrometer. Elemental analyses (C, H, and N) were performed in the University of Florida, Chemistry Department. Chlorine and metal analyses were obtained from Desert Analytics, Tucson, Arizona. Variable-temperature direct current (DC) and alternating current (AC) magnetic susceptibility data were collected on a Quantum Design MPMS-XL SQUID susceptometer equipped with a 7 T magnet and operating in the 1.8−300 K range. Samples were embedded in solid eicosane to prevent torquing. Magnetization versus field and temperature data were fit using the program MAGNET.[11] Pascal's constants[12] were used to estimate the diamagnetic corrections, which were subtracted from the experimental susceptibilities to give the molar paramagnetic susceptibility ($\chi_M$). Cyclic voltammetry (CV) and differential pulse voltammetry (DPV) were performed with a BASi CV50W electrochemistry instrument and a three-electrode cell, using dry MeCN and $NBu^n_4PF_6$ (0.1 M) as supporting electrolyte. A glassy carbon working electrode (BASi model MF-2012) and a coiled platinum wire auxiliary electrode were employed, and the reference electrode was Ag wire; under the same conditions, ferrocene was at 0.18 V versus this reference. The MeCN was distilled over $CaH_2$ and stored over activated molecular sieves. $NBu^n_4PF_6$ was recrystallized in the dark from a $H_2O$/EtOH (1:1 v/v) and dried under vacuum. $^{57}$Fe Mössbauer spectra were obtained at NCSR "Demokritos" and were recorded in the constant acceleration mode at temperatures controlled with a Janis cryostat. Isomer shifts are reported relative to iron metal at room temperature. Simulations of the Mössbauer spectra were obtained with the program WMOSS (See Co., Edina, Minnesota) or with locally written routines.

**Table 1. Crystallographic Data for 1·*x*(solv)**

| | |
|---|---|
| formula[a] | $C_{76}H_{63}Cl_6Fe_{14}O_{31}$ |
| fw, g $mol^{-1}$[a] | 2466.86 |
| crystal system | monoclinic |
| space group | *P*21/*c* |
| *a*, Å | 18.4240(12) |
| *b*, Å | 24.6645(15) |
| *c*, Å | 24.1746(15) |
| $\beta$, deg | 109.349(1) |
| *V*, $Å^3$ | 10364.9(11) |
| *Z* | 4 |
| *T*, K | 173(2) |
| radiation, Å[b] | 0.71073 |
| $\rho_{calc}$, g $cm^{-3}$ | 1.671 |
| $\mu$, $mm^{-1}$ | 2.075 |
| independent reflections | 23599 [*R*(int) = 0.0675] |
| *R*1[c,d] | 0.0406 |
| *wR*2[e] | 0.0831 |

[a] Excluding solvate molecules. [b] Graphite monochromator. [c] $I > 2\sigma(I)$. [d] $R1 = \Sigma||F_o| - |F_c||/\Sigma|F_o|$. [e] $wR2 = [\Sigma w(F_o^2 - F_c^2)^2/\Sigma w(F_o^2)^2]^{1/2}$, $w = 1/[\sigma^2(F_o^2) + [(ap)^2 + bp]$, where $p = [\max(F_o^2, 0) + 2F_c^2]/3$.

## RESULTS AND DISCUSSION

**Synthesis.** The reaction of $fdcH_2$ with iron sources was found to be an extremely complicated one, and many different reaction conditions were explored in developing the procedure to pure, crystalline **1**·*x*(solv) given in the Experimental Section. The use of $FeCl_2$ in MeOH was finally found to give reproducible product in pure form, the MeOH ensuring sufficient solubility of both the $FeCl_2$ and sparingly soluble $fdcH_2$ reagents and, importantly, the product. In addition, the MeOH provided the $MeO^-$ ligand found in **1** (vide infra). After overnight stirring, the reaction was filtered to give a green/blue filtrate and a lot of gray-blue powder. Layering of filtrate with $Et_2O$/hexanes gave well-formed crystals of **1**·*x*(solv) not contaminated with gray-blue powder. A number


dx.doi.org/10.1021/ic200348s |*Inorg. Chem.* 2011, 50, 5646–5654

of other crystallization methods were also explored, but these gave a mixture of crystals and powder, and the two components were determined not to be the same compound, as the color and also IR spectra indicated. The gray-blue powder was essentially insoluble in common solvents and could not be characterized further. The large amount of solvent molecules in $\mathbf{1}\cdot x$(solv) concluded from the crystal structure is consistent with the presence of $Cl^-$ anions and their hydrogen-bonding to solvent molecules. To get an estimate of the content, the crystals were dried very briefly under vacuum, and the elemental analysis (including Cl) was consistent with the formula $\mathbf{1}\cdot 8H_2O\cdot 6$ MeOH. This formulation was used for the magnetism studies (vide infra).

Many different reactions were explored to increase the very low yield of $\mathbf{1}\cdot x$(solv). The formula has a ratio of $fdc^{n-}$ to other Fe of 8:6, but reactions with different $fdcH_2$:$FeCl_2$ ratios showed the optimum ratio to be 2:1; higher or lower ratios giving mixtures of products, often containing both microcrystalline solid and fine powders, including unreacted $fdcH_2$ for the higher ratios. Much of the powder was insoluble in all tested solvents, suggesting polymer formation from $fdc^{2-}$ adopting a bridging mode between different $Fe_7$ or other $Fe_x$ units. The addition of base to deprotonate and solubilize $fdcH_2$ and hopefully increase the yield of **1** also led to mixtures of products as judged from IR spectra and a variety of colored materials. The other products might be completely different compounds from **1**, or other oxidation states of **1**, or both; however, the complexity of the reaction and the obtained mixtures of solids has prevented us from obtaining other compounds in pure form for identification. Mixed solvent systems were also explored, but with no success. For example, a mixed MeOH/MeCN solvent did not have a significant effect on the amount or purity of the product $\mathbf{1}\cdot x$(solv) unless the MeCN was present at >20% (v/v), at which values we obtained decreased and even no amount of crystals of $\mathbf{1}\cdot x$(solv). We, of course, also explored the use $Fe^{III}$ salts as starting materials, but this approach proved unsuccessful; the main product was again an insoluble powder precipitate and no noticeable amount of **1**. We thus in the end were happy to accept very low yields of pure, reproducible material using $FeCl_2$ as the starting material.

It was during the experiments with $FeCl_2$ under different conditions that we noticed the effect of ambient light on $fdcH_2$ reactions. We had already realized that long reaction times were necessary to give the dark green/blue solution color indicative of **1** from the initial orange suspension of $fdcH_2$. Significant darkening of the solution is apparent only after a few hours of stirring, and we thus routinely used long reaction times (~24 h). One reaction mixture was divided into two portions, one of which was kept in room light overnight and the other in the dark. The one exposed to light gave the dark colored solution characteristic of **1**, whereas the other kept its original orange color, and did so for many weeks. This can be attributed to the known photolability of ferrocenyl units substituted with electron-withdrawing groups. Yoshikazu et al.[13] showed how visible light promotes one-electron transitions from the $Fe^{II}$ atom to the cyclopentadienyl unit, which destabilizes the system and can lead to the Fe atom being expelled into the solvent. Something similar is likely occurring in our work, accelerating and directing the reaction toward the formation of **1**, but the heterogeneous nature and complexity of our reaction systems make it difficult to study this in more detail.

However, support for the involvement of photoreleased Fe from $fdcH_2$ under our conditions was obtained by alternative means. When the reaction that gives **1** was explored using $MCl_2$ (M = Mn, Co, Ni, Zn), we again obtained dark colored crystals in low yield. These were found to contain cationic metal cores isomorphous with that of **1**, as determined by IR spectral comparisons and X-ray studies; for M = Mn, a full crystal structure coupled with the results of a complete elemental analysis (C, H, N, Cl, Mn, Fe) revealed the formulation $[Fe_{6.2}Mn_{0.8}O_3(OMe)(fdc)_6(H_2O)_3]Cl$ for the isolated product. We did not analyze in the same detail the isostructural products from the reactions with M = Co, Ni, or Zn, but it seems clear that a similar situation is occurring. This conclusion was confirmed by the $^{57}$Fe Mössbauer spectra of these materials, which are identical to that obtained for the $MnCl_2$ product, all showing the presence of $Fe^{III}$ (vide infra). Since no other iron source was present, it is concluded that the $Fe^{III}$ atoms were derived from $fdcH_2$. We also extended the reaction to larger $Ca^{II}$, $Cd^{II}$, and $Ce^{IV}$ reagents, hoping to crystallographically identify any site preferences for different metals in a mixed-metal product, structurally analogous to **1** or otherwise, but these reactions gave crystalline products that were confirmed by crystallography to be isostructural with **1** and to contain only Fe, that is, they were complex **1**.

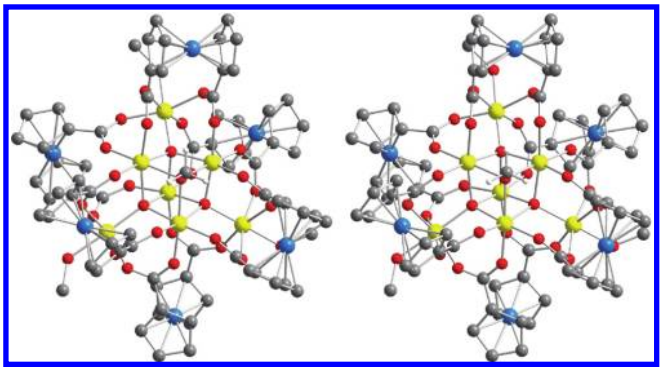

**Figure 1.** Pov-Ray stereopair of the structure of the $[Fe_7O_3(OMe)(fdc)_6(MeOH)_3]^{3+}$ cation of **1**. Hydrogen atoms have been omitted for clarity, except for those on the $\mu_3$-methoxide ion.

**Description of Structure.** A stereopair of the structure of the cation of **1** is shown in Figure 1. The labeled $[Fe_7O_3(OMe)]^{14+}$ core and its interatomic distances and angles are presented in Figure 2 and Table 2, respectively. The cation consists of an $[Fe_7(\mu_4\text{-}O)_3(\mu_3\text{-}OMe)]^{14+}$ core comprising a central cubane whose $O^{2-}$ ions are each also attached to one additional Fe atom; all seven Fe atoms have distorted octahedral geometry. This $[Fe_7(\mu_4\text{-}O)_3(\mu_3\text{-}OMe)]$ core is very similar to the $[Fe_8(\mu_4\text{-}O)_4]$ core of certain $Fe_8$ clusters that differ in having another $O^{2-}$ ion at the $MeO^-$ position of **1**, which thus bridges to an eighth $Fe^{III}$ atom.[14] Peripheral ligation in **1** is provided by six $fdc^{n-}$ groups ($n$ = 1, 2; see below), whose six Fe atoms form a slightly distorted octahedron about the central core, and three MeOH molecules. This gives a complete cation of crystallographic $C_1$ but virtual $C_3$ symmetry, with the virtual rotation axis passing through Fe7 and methoxide atoms O4 and C73. As a result, the $fdc^{n-}$ groups separate into two sets of three by virtual symmetry: One set (Fe9, Fe11, Fe13), those furthest from the methoxide group, bridge four Fe atoms in an $\eta^1{:}\eta^1{:}\eta^1{:}\eta^1{:}\mu_4$ mode with each carboxylate bridging a separate $Fe_2$ pair, whereas the other set (Fe5, Fe8, Fe12) bridges three Fe atoms in a $\eta^1{:}\eta^1{:}\eta^1{:}\eta^1{:}\mu_3$ mode (Figure 3). The ability of the two Cp rings to twist relative to each other clearly assists in this binding flexibility of $fdc^{n-}$: the $\mu_4$ mode has a torsion angle of ~26.7° and thus an almost staggered


dx.doi.org/10.1021/ic200348s |Inorg. Chem. 2011, 50, 5646–5654

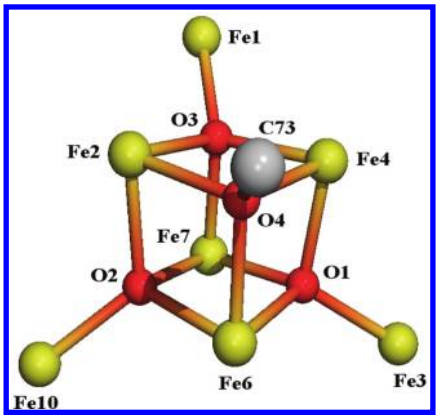


**Figure 2.** Pov-Ray representation of the $[Fe_7O_3(OMe)]^{14+}$ core of the cation of **1** from a viewpoint almost along the virtual $C_3$ axis, emphasizing the three groups of Fe atoms related by virtual symmetry.

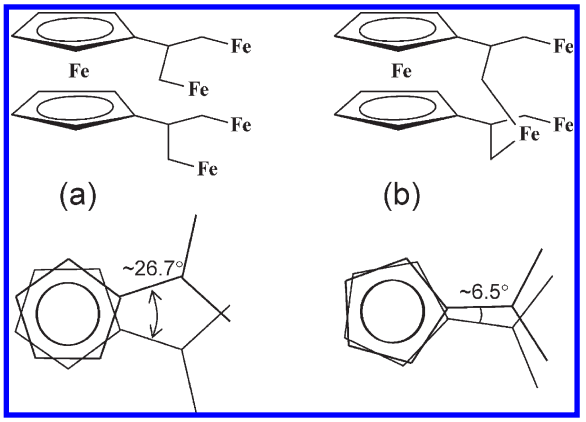


**Figure 3.** Bridging modes and torsion angles for the two sets of $fdc^{n-}$ groups in **1**: (a) the $\mu_4$ groups, with large torsion angles (~26.5°), and (b) the $\mu_3$ groups with small torsion angles (~6.5°).

**Table 2. Selected Interatomic Distances (Å) and Angles (deg) for Complex 1·*x*(solv)**

| | | | |
|---|---|---|---|
| Fe2···Fe4 | 3.156(1) | Fe4···Fe1 | 3.528(1) |
| Fe2···Fe6 | 3.162(1) | Fe4···Fe3 | 3.352(1) |
| Fe2···Fe7 | 3.087(1) | Fe6···Fe3 | 3.490(1) |
| Fe4···Fe6 | 3.119(1) | Fe6···Fe10 | 3.327(1) |
| Fe4···Fe7 | 3.046(1) | Fe7···Fe1 | 3.575(1) |
| Fe6···Fe7 | 3.046(1) | Fe7···Fe3 | 3.609(1) |
| Fe2···Fe1 | 3.341(1) | Fe7···Fe10 | 3.619(1) |
| Fe2···Fe10 | 3.507(1) | Fe4−O4 | 2.077(3) |
| Fe1−O3 | 1.959(3) | Fe6−O1 | 2.042(3) |
| Fe2−O2 | 2.073(3) | Fe6−O2 | 2.011(3) |
| Fe2−O3 | 2.032(3) | Fe6−O4 | 2.101(3) |
| Fe2−O4 | 2.079(3) | Fe7−O1 | 2.063(3) |
| Fe3−O1 | 1.994(3) | Fe7−O2 | 2.079(3) |
| Fe4−O1 | 2.024(3) | Fe7−O3 | 2.075(3) |
| Fe4−O3 | 2.095(3) | Fe10−O2 | 1.985(3) |
| | | | |
| Fe1−O3−Fe2 | 113.71(14) | Fe3−O1−Fe4 | 113.04(13) |
| Fe1−O3−Fe4 | 120.90(14) | Fe3−O1−Fe6 | 119.64(15) |
| Fe1−O3−Fe7 | 124.75(14) | Fe4−O1−Fe6 | 100.18(13) |
| Fe2−O2−Fe6 | 101.46(12) | Fe4−O1−Fe7 | 97.78(12) |
| Fe2−O2−Fe7 | 96.07(12) | Fe4−O3−Fe7 | 95.19(12) |
| Fe2−O2−Fe10 | 119.60(15) | Fe4−O4−Fe6 | 96.61(13) |
| Fe2−O3−Fe4 | 99.74(13) | Fe6−O1−Fe7 | 95.80(12) |
| Fe2−O3−Fe7 | 97.47(12) | Fe6−O2−Fe7 | 96.27(12) |
| Fe2−O4−Fe4 | 98.82(13) | Fe6−O2−Fe10 | 112.79(14) |
| Fe2−O4−Fe6 | 98.29(12) | Fe7−O2−Fe10 | 125.89(16) |
| Fe3−O1−Fe7 | 125.60(14) | | |

$FeCp_2$ conformation (ideal value 36°), whereas the $\mu_3$ mode has a torsion angle of ~6.5° and thus an essentially eclipsed conformation (Figure 3).[15] Ligation at each external Fe atom is completed by a terminal MeOH group. The orientation of the $fdc^{n-}$ groups, and the resulting $C_3$ rather than $C_{3v}$ virtual symmetry, leads to the cation being chiral, and the crystal comprises a racemic mixture of the two enantiomers related by mirror planes (Supporting Information, Figure S1).

The seven non-$fdc^{n-}$ Fe atoms are in the $Fe^{III}$ oxidation state, as suggested by the metric parameters and confirmed by bond valence sum (BVS) calculations,[16] which gave values in the 2.94−3.09 range (Table 3). Given the $[Fe_7O_3(OMe)(fdc)_6(MeOH)_3]^{3+}$ formula of the cation, this indicates that one of the ligands is in the oxidized $fdc^-$ oxidation level, the remainder being $fdc^{2-}$; in fact, at least one oxidized ligand was expected from the blue color of the cation, which is not a color expected for Fe/O clusters but which is characteristic of the ferricenium cation, $Cp_2Fe^+$. The BVS approach is not reliable for assigning the $Fe^{II}/Fe^{III}$ oxidation state within such an organometallic unit, and we instead looked at other distances within **1** to probe this point. Oxidation of a free ferrocene unit to ferricenium leads to a lengthening of the centroid-centroid distance (centroid = CT = the center of the Cp ring) by <0.1 Å on average,[17] which is a small change. Substituents on the rings and binding to additional metal centers will affect these changes. Shown in Table 4 are the Fe-CT and CT-CT distances in **1**, and we see that neither parameter shows any major difference that could be assigned to clearly being in the oxidized state. The distances at Fe12 do show slightly longer values, but these differences are statistically borderline. We conclude that although (i) the blue color of the crystal clearly indicates that **1** contains an oxidized (ferricenium-containing) $fdc^-$ ligand, as supported by the UV/vis spectral comparison between **1** and $(Cp_2Fe)(PF_6)$ shown in Supporting Information, Figure S2, and (ii) distances at Fe12 are slightly longer than those at other ferrocenyl Fe atoms, there is nevertheless no unequivocal statistical evidence from the structural parameters for one of the ligands being in

**Table 3. Bond Valence Sums for the Non-Ferrocene Fe atoms in 1[a]**

| atom | $Fe^{II}$ | $Fe^{III}$ |
|---|---|---|
| Fe1 | 2.88 | 3.08 |
| Fe2 | 2.77 | 2.96 |
| Fe3 | 2.79 | 2.99 |
| Fe4 | 2.80 | 2.99 |
| Fe6 | 2.89 | 3.09 |
| Fe7 | 2.75 | 2.94 |
| Fe10 | 2.79 | 2.99 |
| Fe14[b] | 2.87 | 3.11 |

[a] The value underlined is the closest to the charge for which it was calculated; the oxidation state of that atom is the nearest integer to the underlined value. [b] $[FeCl_4]^-$ anion.


dx.doi.org/10.1021/ic200348s |*Inorg. Chem.* 2011, 50, 5646–5654

**Table 4. Fe-Centroid and Centroid-Centroid Distances[a] in 1**

| atom | Fe-CT[b,c] | CT-CT[b,d] |
|---|---|---|
| Fe5[e] | 1.636, 1.652 | 3.288 |
| Fe8[e] | 1.645, 1.652 | 3.297 |
| Fe12[e] | 1.656, 1.659 | 3.314 |
| Fe9[f] | 1.646, 1.640 | 3.287 |
| Fe11[f] | 1.649, 1.650 | 3.299 |
| Fe13[f] | 1.647, 1.653 | 3.299 |
| average | 1.649 | 3.297 |

[a] In Å. [b] CT = centroid. [c] ±0.001 Å. [d] ±0.002 Å. [e] Related by virtual symmetry. [f] Related by virtual symmetry.

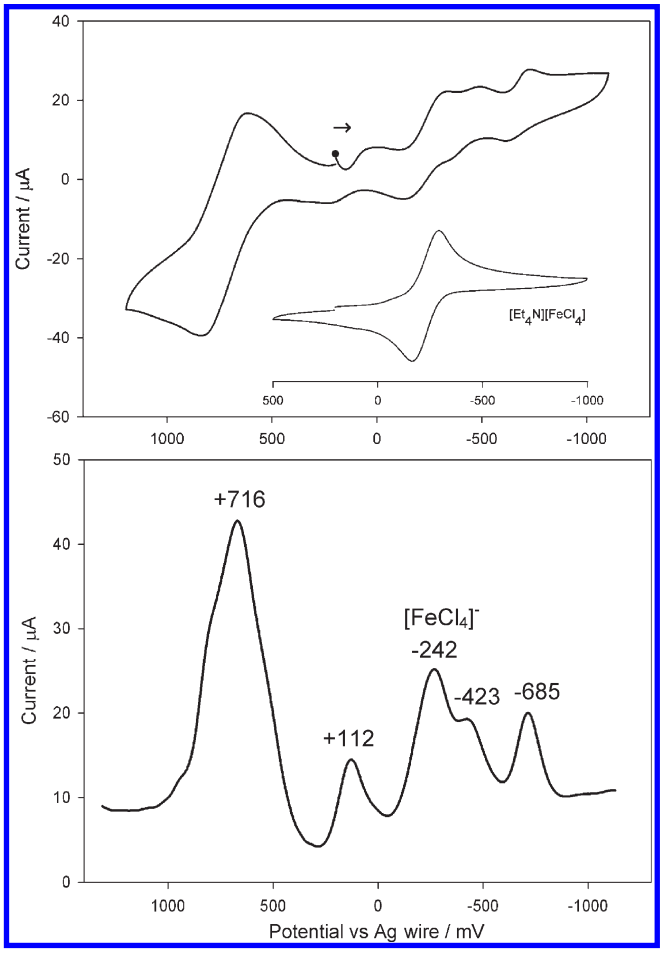


**Figure 4.** CV at 100 mV/s (top) and DPV at 20 mV/s (bottom) for complex **1** in dry MeCN containing 0.10 M $NBu^n_4PF_6$ as supporting electrolyte, showing the multielectron oxidations at +0.716 V and the three one-electron reductions at +112, −423, and −685 V. The CV of $(NEt_4)[FeCl_4]$ under the same conditions is shown as an inset in the top figure.

the oxidized ($fdc^-$) level. This is, of course, consistent with the only small changes expected on oxidation and the possibility in **1** of static disorder of the oxidized ligand among the three groups related by virtual symmetry, and even among all six of them.

**Electrochemistry.** A freshly prepared crystalline sample of **1** was dried well under vacuum before being used. The compound is only slightly soluble in the electrochemical solvent, and the solution reached saturation at less than the intended 1 mM concentration. The cyclic voltammogram (CV) at 100 mV/s and the differential pulse voltammogram (DPV) at 20 mV/s are shown in Figure 4, top and bottom, respectively. The compound exhibits a wealth of quasi-reversible features. There are four reversible reductions, two of which overlap, but they nevertheless appear to all involve one-electron processes; the second reduction was identified as due to the $[FeCl_4]^-$ anion by comparison with the plots of $[NEt_4][FeCl_4]$ in the same solvent. In addition, on the oxidizing side there is a large, clearly multielectron feature assignable to oxidation of the $fdc^{2-}$ groups. There was a spike in the current when the potential of +195 mV (vs $fc/fc^+$) was first applied to the cell, which we assign as reduction at this potential of the one oxidized $fdc^-$ ligand. Thus, the multielectron oxidation should be due to the six one-electron oxidations of the $fdc^{2-}$ groups. Their overlap within the resolution of the CV experiment is consistent with the $fdc^{2-}$ groups behaving near-independently and thus being oxidized at essentially the same potentials. This is supported by the relative peak current heights, although the ratio of the oxidation versus the reduction features is closer to 10:1 rather than 6:1, probably because of different electron transfer kinetics from the outer $fdc^{2-}$ redox sites than to the inner ones. A difference is also seen between the relative size of the $[FeCl_4]^-$ and cation reductions, which will also be affected by differing diffusion coefficients.

DPV is better at resolving overlapping features and allowing potentials to be determined. The latter are shown on the DPV plot versus Ag wire; the ferrocene couple was measured at +180 mV versus this reference under the same conditions. The DPV plot also shows shoulders on the large multielectron oxidation peak confirming it to be composed of poorly resolved separate features, consistent with the two sets of $fdc^{2-}$ groups by symmetry and some small electronic communication between the various groups. Including the six $fdc^{-/2-}$ ligands, the cation of **1** can thus electrochemically access 10 oxidation levels, from the fully oxidized all-$Fe^{III}$ complex $[Fe^{III}_7(fdc^-)_6]^{15+}$, through the $[Fe^{III}_7(fdc^{2-})_5(fdc^-)]^{10+}$ level of complex **1**, to the $[Fe^{III}_4Fe^{II}_3(fdc^{2-})_6]^{6+}$ reduced level.

**Magnetochemistry.** Variable-temperature magnetic susceptibility measurements were performed on microcrystalline powder samples of complex $\mathbf{1}\cdot 8H_2O\cdot 6MeOH$ in a 1 kOe (0.1 T) DC field in the 5.0−300 K range. The sample was restrained in eicosane to prevent torquing in the applied field. The obtained data are shown as a $\chi_M T$ versus $T$ plot in Figure 5. $\chi_M T$ decreases steadily from 16.39 $cm^3$ K $mol^{-1}$ at 300 K to 7.56 $cm^3$ K $mol^{-1}$ at 40 K, below which it is essentially constant. These values include the contribution from the high-spin $[FeCl_4]^-$ anion ($S = {}^5/_2$, $\chi_M T$ = 4.38 $cm^3$ K $mol^{-1}$ for $g$ = 2.0). To determine the $\chi_M T$ versus $T$ values for the cation, we prepared $[NEt_4][FeCl_4]$[18] and collected its $\chi_M T$ versus $T$ data (Figure 5), which were subtracted from those of $\mathbf{1}\cdot 8H_2O\cdot 6MeOH$. This approach assumes only minimal exchange interactions between the cations and the anions, which is supported by the crystal structure; only weak Cl···H−C contacts to Cp rings are observed. The resulting data for the cation show $\chi_M T$ to be 11.62 $cm^3$ K $mol^{-1}$ at 300 K decreasing to 3.17 $cm^3$ K $mol^{-1}$ at 40 K, below which $\chi_M T$ increases again to 4.37 $cm^3$ K $mol^{-1}$ at 1.8 K. However, the latter is very likely an artifact of the subtraction of the $[NEt_4][FeCl_4]$ data at these lowest temperatures, which show a significant decrease below 40 K assignable to inter-$[FeCl_4]^-$ interactions. We thus took the 40 K value of 3.17 $cm^3$ K $mol^{-1}$ as the low-temperature plateau value for the cation of $\mathbf{1}\cdot 8H_2O\cdot 6MeOH$ (which differs by 4.39 $cm^3$ K $mol^{-1}$ from that of the

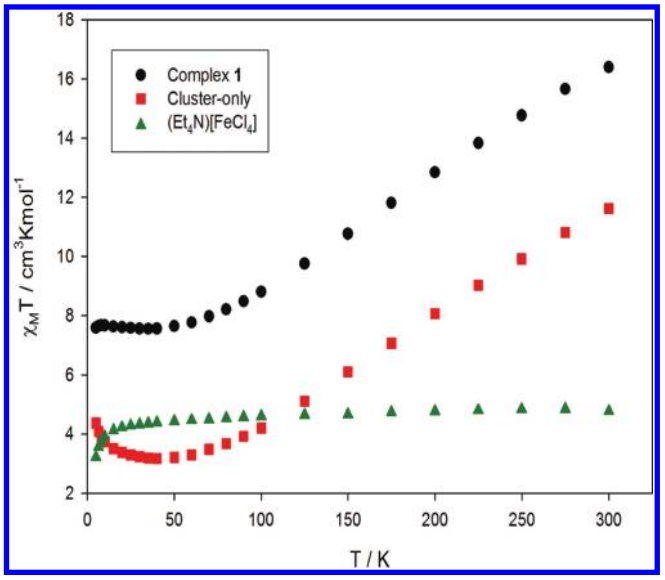


**Figure 5.** Plots of DC $\chi_M T$ vs $T$ for complex $\mathbf{1}\cdot 8H_2O\cdot 6MeOH$ and $[NEt_4][FeCl_4]$ using data collected at 1.0 kOe. The difference plot, corresponding to the $\chi_M T$ vs $T$ for the $Fe_7$ cluster, is also shown.

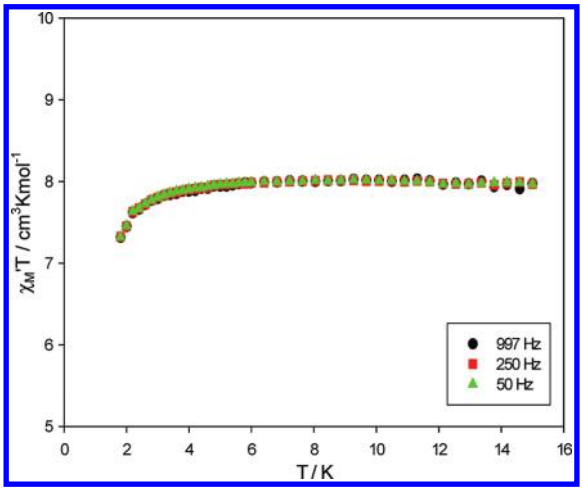


**Figure 6.** In-phase ($\chi_M'$, plotted as $\chi_M'T$ vs $T$) AC susceptibility of complex $\mathbf{1}\cdot 8H_2O\cdot 6MeOH$ in a 3.5 Oe field oscillating at the indicated frequencies.

anion−cation pair, the expected value for the anion). The cation value indicates an $S = 2$ ground state with $g \approx 2.05$.

The $\chi_M T$ versus $T$ profile for the cation indicates strong antiferromagnetic interactions within the $Fe^{III}_7$ core, and the $S = 2$ ground state is as expected for antiferromagnetic coupling between an $S = {}^5/_2$ $Fe_7$ unit and one $S = {}^1/_2$ oxidized $fdc^-$ ligand. The $g$ slightly >2 is reasonable for high-spin $Fe^{III}$, and especially since the oxidized ferricenyl group generally has $g > 2$.[19] Given the low symmetry of the cationic cluster and the relatively large number of metal atoms and independent pairwise exchange parameters ($J_{ij}$) describing the exchange couplings, we did not pursue the fitting of the $\chi_M T$ versus $T$ data by matrix diagonalization. For symmetry reasons, the convenient Kambe vector coupling method is not applicable.[20]

As an independent determination of the ground state, we also carried out AC susceptibility studies, which preclude any complications from an applied DC field. Data were obtained for the 1.8−15 K range using a 3.5 Oe AC field oscillating at frequencies in the 50−1000 Hz range. In the absence of slow magnetization relaxation and thus no out-of-phase ($\chi_M''$) AC susceptibility signal, the in-phase $\chi_M'T$ is equal to the DC $\chi_M T$, allowing determination of the ground state $S$ in the absence of a DC field. Complex $\mathbf{1}\cdot 8H_2O\cdot 6MeOH$ was indeed found to exhibit no $\chi_M''$ signal (Supporting Information, Figure S3).

The $\chi_M'T$ versus $T$ plot is shown in Figure 6. It is essentially temperature-independent at ~8.0 $cm^3\ K\ mol^{-1}$ down to ~5 K, below which it decreases slightly to ~7.3 $cm^3\ K\ mol^{-1}$. The latter decrease is assigned to a combination of weak inter-ion exchange interactions and zero-field splitting. Subtracting the estimated contribution of the $[FeCl_4]^-$ anion of 4.38 $cm^3\ K\ mol^{-1}$ leaves a value of ~3.6 $cm^3\ K\ mol^{-1}$. This is somewhat higher than that obtained from the DC analysis above (3.1 $cm^3\ K\ mol^{-1}$), no doubt because of the experimental error and the approximations made, but still clearly indicates an $S = 2$ ground state with $g > 2.0$; $S = 1$ or 3 states would give $\chi_M'T$ of 1.0 and 6.0 $cm^3\ K\ mol^{-1}$, respectively, for $g = 2.0$, and slightly higher for $g > 2$. We thus conclude that an $S = 2$ ground state is confirmed.[21]

**$^{57}$Fe Mössbauer Spectroscopy.** Complex **1** represents a challenging case to study by $^{57}$Fe Mössbauer spectroscopy because of the complexity of its structure and the many inequivalent iron sites by virtual symmetry and oxidation level. The spectrum was consequently expected to be rather rich and complicated. According to the molecular formula and the structure of the compound, the following features were expected:

(a) Five $Fe^{II}$ ferrocenyl sites within the $fdc^{2-}$ ligands. These moieties give rise to characteristic narrow doublets with isomer shift of ~0.5 mm $s^{-1}$ at 78 K and quadrupole splitting $\Delta E_Q > 2.0$ mm $s^{-1}$.[22]

(b) One $Fe^{III}$ ferricenium site within the $fdc^-$ ligand. For these, $\Delta E_Q$ is relatively small.[22] In pure ferricenium complexes, $\Delta E_Q \approx 0.0$ mm $s^{-1}$ whereas in mixed-valence complexes in a trapped-valence situation, $\Delta E_Q \approx 0.4$ mm/s for the ferricenium moiety.[23]

(c) Seven high-spin $Fe^{III}$ sites of the octahedral $FeO_6$ type. The isomer shift is expected to be 0.45−0.50 mm $s^{-1}$ at 78 K with a moderate $\Delta E_Q$ (≈ 0.4−0.6 mm $s^{-1}$).[22]

(d) One $Fe^{III}$ site within the $[FeCl_4]^-$ anion. The isomer shift of this four-coordinate high-spin ferric site is expected to be smaller than that of the octahedral sites, and with a negligible $\Delta E_Q$.[24]

Thus, we expected that the Fe sites that would most readily be resolved by $^{57}$Fe Mössbauer spectroscopy would be the five $fdc^{2-}$ groups because of their large $\Delta E_Q$. We expected that it would be more difficult to resolve the $fdc^-$ and the $[FeCl_4]^-$ contributions because of their low content (~7% each).

Variable-temperature, zero-field Mössbauer spectra are shown in Figure 7; the 185 and 250 K spectra are expanded in Supporting Information, Figure S4. At 250 K, the spectrum consists of two quadruple doublets. The outer doublet exhibits well resolved lines at −0.62 and +1.56 mm $s^{-1}$ with relatively small line-widths (fwhm ≈0.25 mm $s^{-1}$, very close to the limits of the instrument used), and its parameters and relative contribution to the total spectrum can thus be determined with high accuracy. The isomer shift (0.48 ± 0.02 mm $s^{-1}$) and quadruple splitting (2.16 ± 0.02 mm $s^{-1}$) are characteristic of ferrocene, and this doublet is assigned to the $fdc^{2-}$ ligands. The relatively small line width of the doublet suggests that $\Delta E_Q$ of the ferrocene


dx.doi.org/10.1021/ic200348s |Inorg. Chem. 2011, 50, 5646–5654

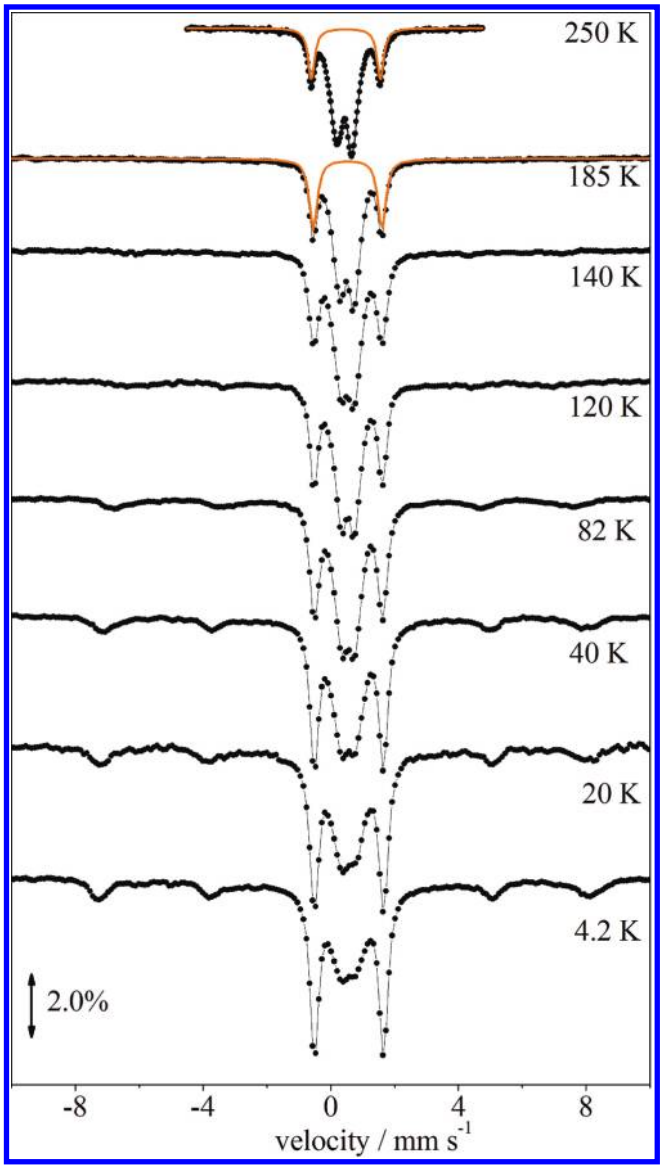


**Figure 7.** $^{57}$Fe Mössbauer spectra in zero applied field for powder samples of **1** in the 4.2−250 K temperature range. The contribution of the ferrocene doublet is shown with the orange line.

species is not sensitive to the relative orientation of the rings, in agreement with theoretical calculations.[25]

The rest of the spectrum consists of a relatively broad, asymmetric doublet with peaks at +0.20 and +0.65 mm s$^{-1}$ with an average isomer shift of ∼0.40 mm s$^{-1}$ and average quadruple splitting of ∼0.45 mm s$^{-1}$. This part of the spectrum is expected to contain contributions from the seven $FeO_6$ sites and the $[FeCl_4]^-$ and ferricenium moieties. However, no special features can be resolved that could lead to an unambiguous discrimination of the different $Fe^{III}$ species.

The doublet attributed to the ferrocene site of $fdc^{2-}$ accounts for only 22% of total iron at 250 K, which is significantly lower than the expected value of ∼36% for five $fdc^{2-}$ ligands per molecule. This cannot be due to only three $fdc^{2-}$ ligands per molecule (predicted 21% of total Fe) because this would be completely inconsistent with the other data. We instead believe that this is due to the various iron sites being characterized by different Debye−Waller factors. Such effects have been seen, for example, in biferricenium complexes, where the ferrocene Debye−Waller factor has been reported to be smaller than other Fe sites at higher temperatures.[26] In other words, the Debye−Waller for the ferrocene groups in **1** is smaller and their contribution is thus underestimated in comparison with the other iron sites at elevated temperatures. Indeed, as the temperature decreases the contribution of the $fdc^{2-}$ ferrocene doublet increases and below 20 K accounts for ∼36% of total iron, the expected percentage for five $fdc^{2-}$ per molecule. The quadruple splitting for the $fdc^{2-}$ ferrocene doublet does not exhibit any temperature dependence, and the lines remain narrow. Therefore, the liquid helium spectra provide compelling evidence that **1** contains five ferrocene ($fdc^{2-}$) and one ferricenium ($fdc^-$) groups.[21]

Below 120−140 K, the rest of the spectrum exhibits a rather unexpected behavior. As the temperature decreases, the central doublet loses intensity, and this decrease is accompanied by the development of a magnetically split spectrum (sextet). It is important to emphasize this; the sextet gains intensity as the central doublet loses it, that is, the relative area ratio of the ferrocene doublet and the other features combined at liquid He temperatures remains that predicted by the crystal structure of **1**. This thus excludes the possibility that the sextet is due to iron impurities, and that it could not be observed at higher temperatures because of broadening effects, or similar. The iron sites that contribute to the sextet are thus among the ferric sites of the $Fe_7$ core and/or the ferricenium site. The $[FeCl_4]^-$ anion is not expected to contribute to the sextet because of its minimal interactions with the cation, and it is thus unlikely that there are significant anion/cation exchange interactions; this was also inferred from the magnetic susceptibility measurements above. Because of fast spin relaxation, the $[FeCl_4]^-$ anion in complex salts gives rise to a Mössbauer singlet with $\delta \sim 0.35$ mm s$^{-1}$ at liquid helium temperatures and above.[27] In the present case, the singlet from the $[FeCl_4]^-$ anion accounts for only 7% of total iron and would be buried under the central doublet. As a consequence, we believe that the sextet arises from magnetic interactions within the $Fe_7$ core, involving also the $S = {}^1/_2$ ferricenium group.

The sextet is rather broad even at 4.2 K, and the resolution of the spectra does not allow us to identify the contribution of each ferric site. Each of the four types of $Fe^{III}$ sites is expected to be characterized by different hyperfine fields, and this, in combination with possible relaxation effects, would result in substantial line broadening. Rough simulations of the spectra were carried out to estimate the average hyperfine fields of the magnetic sextets. The temperature dependence of (i) the average hyperfine field of the magnetic sextet, and (ii) the percentage of magnetic sextet relative to the central doublet, are shown in Supporting Information, Figures S5 and S6, respectively. The average hyperfine field exhibits an apparent increase down to 20 K and then remains constant (Supporting Information, Figure S5). The gradual conversion of the central doublet to the magnetic sextet does not follow the behavior expected for typical slow relaxation as it is manifested in other polynuclear iron clusters.[29] Rather, the behavior of the spectra of **1** is reminiscent of systems with spin correlations, but the magnetic susceptibility measurements do not indicate long-range magnetic ordering. Interestingly, similar behavior was observed recently for a $Dy^{III}{}_3Fe^{III}{}_7$ cluster whose zero-field Mössbauer spectra on powder samples below 15 K exhibit magnetic sextets with temperature-dependent hyperfine fields.[29] The behavior of the Mössbauer


dx.doi.org/10.1021/ic200348s |*Inorg. Chem.* 2011, 50, 5646–5654

spectra of **1** is possibly related to the increasing thermal population of spin state manifolds with slow relaxation properties (on the Mössbauer time scale) as the temperature decreases. In any event, the exact mechanism for this behavior is not fully understood, and it warrants more thorough investigation. We note, however, that in comparison with the $Dy^{III}{}_3Fe^{III}{}_7$ cluster, the magnetically split spectra in **1** emerge at significantly higher temperatures (~120−140 K).

The 78 K Mössbauer spectra of the complexes derived from the $MCl_2$ (M = Mn, Co, Ni, Zn) salts are shown in the Supporting Information, Figure S7. The spectra are almost identical and consist of two distinct doublets with parameters consistent with $fdc^{2-}$ groups ($\delta$ = 0.51 mm $s^{-1}$, $\Delta E_Q$ ~ 2.22−2.23 mm $s^{-1}$) and high-spin $Fe^{III}$ sites ($\delta$ ~ 0.51 mm $s^{-1}$, $\Delta E_Q$ ~ 0.45−0.51 mm $s^{-1}$)) (Supporting Information, Table S1). For all the clusters, the ratio of $fdc^{2-}$ to high-spin $Fe^{III}$ is 45:55 at 80 K, indicating little or no $fdc^-$ in the compounds. Because $fdc^{2-}$ is the only iron source in the reaction, the high-spin $Fe^{III}$ must all derive from dissociation of iron from $fdc^{2-}$, as discussed earlier. Moreover, the extremely similar spectra suggest the product of each reaction depends little on the $MCl_2$ salt employed. Thus, they likely all have a similar M:Fe content (excluding $fdc^{2-}$/$fdc^-$) as the product from $MnCl_2$, which analyzed with Mn:Fe ~ 0.8:6.2, that is, approximately one M per cation. The absence of a magnetic sextet in these spectra further suggests that the oxidized $fdc^-$ ferricenium ligand of **1** plays a significant role in yielding the sextet for that compound.

## CONCLUSIONS

The reactions of $fdcH_2$ with $Fe^{II}$ or $Fe^{III}$ sources have proved to be very challenging because of the formation of amorphous precipitates that are essentially insoluble in all inert solvents. This is probably due to the formation of polymeric products, a situation that is commonly encountered in the chemistry of $fdc^{2-}$. However, it should also be noted that neutral molecular compounds of $fdc^{2-}$ are also often very insoluble, such as $[Mn_{13}O_8(OEt)_6(fdc)_6]$,[3c,7] which has unfortunately precluded their study in solution. Nevertheless, the slow reaction of $fdcH_2$ with $FeCl_2$ also gives a more soluble fraction that was crystallized and characterized as **1**·solv. The solubility is undoubtedly assisted by its cationic nature. The photorelease of Fe from $fdcH_2$ was shown to occur and give **1** or mixed-metal analogues when other metal reagents were employed; in fact, there are literature studies attempting to characterize the photodecomposition products of $fdcH_2$[30−33] and, under our conditions at least, they drive the formation of the cation of **1**.

The unusual nature of **1** was immediately evident from its blue color, and we conclude from the various data that it contains one oxidized $fdc^-$ ligand. This is the first structurally characterized example to our knowledge of this ligand in inorganic chemistry. There is one other claim of a $fdc^-$ ligand, in the compounds $[Zn_6O_2(fdc)_5(H_2O)(DMF)]$ and $[Zn_8O_4(fdc)_6(H_2O)_3]$ made by hydrothermal reaction of $fdcH_2$ with $Zn(NO_3)_2$; however, the reported magnetic data and the dark red color are not consistent with $fdc^-$, and our suspicion is that some of the Zn sites are occupied by $Fe^{III}$ released from $fdc^{2-}$ under the high energy reaction conditions.[3b]

The electrochemical studies indicate a new class of compound that has rich redox behavior, and we are excited by the possibility that the $Fe_7$ cation could be generated, isolated, and characterized at different oxidation levels. However, this requires a route to greater amounts of **1** than are currently available. The latter is also important to allow study in more detail of the unusual low-temperature Mössbauer spectra and elucidate the precise origin of the sextet signal. In summary, our preliminary work has convinced us that the incorporation of multiple $fdc^{n-}$ ligands into magnetic metal clusters has the potential for interesting new magnetic and redox behavior, and work along these lines is continuing.

## ASSOCIATED CONTENT

**Supporting Information.** X-ray crystallographic data in CIF format for complex **1**·*x*(solv), AC magnetic data, and Mössbauer spectra and tables. This material is available free of charge via the Internet at http://pubs.acs.org.

## AUTHOR INFORMATION

**Corresponding Author**

*Phone: +1-352-392-8314. Fax: +1-352-392-8757. E-mail: christou@chem.ufl.edu.

## ACKNOWLEDGMENT

We thank the National Science Foundation (CHE-0910472) for support of this work.

## REFERENCES

(1) (a) Christou, G.; Gatteschi, D.; Hendrickson, D. N.; Sessoli, R. *MRS Bull* **2000**, *25*, 66. (b) Sessoli, R.; Tsai, H.-L.; Schake, A. R.; Wang, S.; Vincent, J. B.; Folting, K.; Gatteschi, D.; Christou, G.; Hendrickson, D. N. *J. Am. Chem. Soc.* **1993**, *115*, 1804. (c) Caneschi, A.; Gatteschi, D.; Sessoli, R.; Barra, A. L.; Brunel, L. C.; Guillot, M. *J. Am. Chem. Soc.* **1991**, *113*, 5873.

(2) (a) Stamatatos, T. C.; Christou, G. *Inorg. Chem.* **2009**, *48*, 3308–3322. (b) Stamatatos, T. C.; Vinslava, A.; Abboud, K. A.; Christou, G. *Chem. Commun.* **2009**, 2839–2841.

(3) (a) Meng, X.; Hou, H.; Li, G.; Ye, B.; Ge, T.; Fan, Y.; Zhu, Y.; Sakiyama, H. *J. Organomet. Chem.* **2004**, *689*, 1218. (b) Kim, Y. S.; Kim, J.; Kim, D.; Chae, H. K. *Chem. Lett.* **2007**, *36*, 150. (c) Dong, G.; Li, Y.-T.; Duan, C.-Y.; Hong, M.; Meng, Q.-J. *Inorg. Chem.* **2003**, *42*, 2519. (d) Kondo, M.; Shinagawa, R.; Miyazawa, M.; Kabir, M. K.; Irie, Y.; Horiba, T.; Naito, T.; Maeda, K.; Utsuno, S.; Uchida, F. *Dalton Trans.* **2003**, *4*, 515. (e) Cowley, A. R.; Hector, A. L.; Hill, A. F.; White, A. J. P.; Williams, D. J.; Wilton-Ely, J. D. E. T. *Organometallics* **2007**, *26*, 6114. (f) Wang, L.; Meng, X.; Zhang, E.; Hou, H.; Fan, Y. *J. Organomet. Chem.* **2007**, *692*, 4367. (g) Mereacre, V.; Prodius, D.; Ako, A. M.; Shova, S.; Turta, C.; Wurst, K.; Jaitner, P.; Powell, A. K. *Polyhedron* **2009**, *28*, 3551. (h) Kuehnert, J.; Rueffer, T.; Ecorchard, P.; Braeuer, B.; Lan, Y.; Powell, A. K.; Lang, H. *Dalton Trans.* **2009**, *23*, 4499.

(4) (a) Lee, S.-M.; Cheung, K.-K.; Wong, W.-T. *J. Organomet. Chem.* **1996**, *506*, 77. (b) Cotton, F. A.; Lin, C.; Murillo, C. A. *Inorg. Chem.* **2001**, *40*, 478. (c) Maksakov, V. A.; Slovohotova, I. V.; Golovin, A. V.; Babailov, S. P. *Russ. Chem. Bull* **2001**, *50*, 2451. (d) Bera, J. K.; Clerac, R.; Fanwick, P. E.; Walton, R. A. *Dalton Trans.* **2002**, *10*, 2168. (e) Das, N.; Arif, A. M.; Stang, P. J.; Sieger, M.; Sarkar, B.; Kaim, W.; Fiedler, J. *Inorg. Chem.* **2005**, *44*, 5798.

(5) (a) Meng, X.; Li, G.; Hou, H.; Han, H.; Fan, Y.; Zhu, Y.; Du, C. *J. Organomet. Chem.* **2003**, *679*, 153. (b) Mereacre, V.; Ako, A. M.; Filoti, G.; Bartolome, J.; Anson, C. E.; Powell, A. K. *Polyhedron* **2010**, *29*, 244. (c) Wen, L.-L.; Zhang, B.-G.; Peng, Z.-H.; Ren, J.-G.; Cai, P.; Duan, C.-Y. *Wuji Huaxue Xuebao* **2004**, *20*, 1228.

(6) (a) Uhl, W.; Spies, T.; Haase, D.; Winter, R.; Kaim, W. *Organometallics* **2000**, *19*, 1128. (b) Meng, X.; Cheng, W.; Mi, L.; Tang, M.; Hou, H. *Inorg. Chem. Commun.* **2006**, *9*, 662. (c) Guo, D.; Zhang, B.-g.;

Duan, C.-Y.; Cao, X.; Meng, Q.-J. *Dalton Trans.* **2003**, *3*, 282. (d) Chandrasekhar, V.; Thirumoorthi, R. *Organometallics* **2007**, *26*, 5415. (e) Zheng, G.; Ma, J.; Su, Z.; Yan, L.; Yang, J.; Li, Y.; Liu, J. *Angew. Chem., Int. Ed.* **2004**, *43*, 2409.

(7) Masello, A.; Murugesu, M.; Abboud, K. A.; Christou, G. *Polyhedron* **2007**, *26*, 2276.

(8) *SHELXTL6*; Bruker-AXS: Madison, WI, 2000.

(9) Van der Sluis, P.; Spek, A. L. *Acta Crystallogr., Sect. A* **1990**, *A46*, 194.

(10) *PLATON*; Spek, A. L. *Acta Crystallogr.* **1990** *A46*, C-34.

(11) Davidson, E. R. *MAGNET*; Indiana University: Bloomington, IN, 1999.

(12) Weast, R. C. *CRC Handbook of Chemistry and Physics*; CRC Press, Inc.: Boca Raton, FL, 1984.

(13) Yamaguchi, Y.; Ding, W.; Sanderson, C. T.; Borden, M. L.; Morgan, M. J.; Kutal, C. *Coord. Chem. Rev.* **2007**, 240.

(14) (a) Raptis, R. G.; Georgakaki, I. P.; Hockless, D. C. R. *Angew. Chem., Int. Ed.* **1999**, *38*, 1632. (b) Baran, P.; Boca, R.; Chakraborty, I.; Giapintzakis, J.; Herchel, R.; Huang, Q.; McGrady, J. E.; Raptis, R. G.; Sanakis, Y.; Simopoulos, A. *Inorg. Chem.* **2008**, *47*, 645. (c) Chakraborty, I.; Baran, P.; Sanakis, Y.; Simopoulos, A.; Fachini, E.; Raptis, R. G. *Inorg. Chem.* **2008**, *47*, 11734. (d) Gass, I. A.; Milios, C. J.; Whittaker, A. G.; Fabiani, F. P. A.; Parsons, S.; Murrie, M.; Perlepes, S. P.; Brechin, E. K. *Inorg. Chem.* **2006**, *45*, 5281. (e) Hahn, F. E.; Jocher, C.; Lugger, T. *Z. Naturforsch.* **2004**, *59*, 855.

(15) *IUPAC, Compendium of Chemical Terminology*, 2nd ed.; Blackwell Science: Oxford, U.K., 1997.

(16) Kanowitz, S. M.; Palenik, G. J. *Inorg. Chem.* **1998**, *37*, 2086.

(17) (a) Cowan, D. O.; Shu, P.; Hedberg, F. L.; Rossi, M.; Kistenmacher, T. J. *J. Am. Chem. Soc.* **1979**, *101*, 1138. (b) Bats, J. W.; Scheibitz, M.; Wagner, M. *Acta Crystallogr., Sect. C.* **2003**, *C59*, 355.

(18) Walters, M. A.; Chaparro, J.; Siddiqui, T.; Williams, F.; Ulku, C.; Rheingold, A. L. *Inorg. Chim. Acta* **2006**, *359*, 3996.

(19) Duggan, D.; Michael; Hendrickson, D. N. *Inorg. Chem.* **1975**, *14*, 955.

(20) Kambe, K. *J. Phys. Soc. Jpn.* **1950**, *5*, 48.

(21) We cannot rule out the possibility that in addition to **1**, which contains five $fdc^{2-}$ and one $fdc^{-}$ (5/1), the crystals might be contaminated with small amounts of the 6/0 or 4/2 variants, but both would have to be present, and in approximately equal amounts, or it would have affected the obtained magnetism and Mossbauer data noticeably.

(22) Greenwood, N.N.; Gibb, T.C. In *Mössbauer Spectroscopy*; Chapman and Hall Ltd: London, U.K., 1971.

(23) Morrison, W. H., Jr.; Hendrickson, D. N. *Inorg. Chem.* **1975**, *14*, 2331.

(24) Edwards, P. R.; Johnson, C. E. *J. Chem. Phys.* **1968**, *49*, 211.

(25) Nemykin, V. N.; Hadt, R. G. *Inorg. Chem.* **2006**, *45*, 8297.

(26) Jiao, J.; Long, G. J.; Rebbouh, L.; Grandjean, F.; Beatty, A. M.; Fehlner, T. P. *J. Am. Chem. Soc.* **2005**, *127*, 17819.

(27) Witten, E. H.; Reiff, W. M.; Lazar, K.; Sullivan, B. W.; Foxman, B. M. *Inorg. Chem.* **1985**, *24*, 4585.

(28) (a) Barra, A. L.; Debrunner, P.; Gatteschi, D.; Schulz, C. E.; Sessoli, R. *Europhys. Lett.* **1996**, *35*, 133. (b) Cianchi, L.; Del Giallo, F.; Spina, G.; Reiff, W.; Caneschi, A. *Phys. Rev. B* **2002**, *65*, 064415. (c) Van Slageren, J.; Rosa, P.; Caneschi, A.; Sessoli, R.; Caellas, H.; Ratikin, Y. V.; Cianchi, L.; Del Ciallo, F.; Spina, G.; Bino, A.; Barra, A.-L.; Guidi, T.; Caretta, S.; Caciuffo, R. *Phys. Rev. B* **2006**, *73*, 014422. (d) Boudalis, A. K.; Sanakis, Y.; Clemente-Juan, J. M.; Donnadieu, B.; Nastopoulos, V.; Tuchagues, J.-P.; Perlepes, S. P. *Chem.—Eur. J.* **2008**, *14*, 2514.

(29) Abbas, G.; Lan, Y.; Mereacre, V.; Wernsdorfer, W.; Clerac, R.; Buth, G.; Sougrati, M. T.; Grandjean, F.; Long, G. J.; Anson, C. E.; Powell, A. K. *Inorg. Chem.* **2009**, *48*, 9345.

(30) Bergamini, P.; Di Martino, S.; Maldotti, A.; Sostero, S.; Traverso, O. *J. Organomet. Chem.* **1989**, *365*, 341.

(31) Ali, L. H.; Cox, A.; Kemp, T. J. *J. Chem. Soc., Dalton Trans.* **1973**, *14*, 1468.

(32) Che, D.-J.; Li, G.; Yao, X. L.; Zou, Da P. *J. Organomet. Chem.* **1998**, *568*, 165.

(33) Che, D.-J.; Li, G.; Du, B.-S.; Zhang, Z.; Li, Y. H. *Inorg. Chim. Acta* **1997**, *261*, 121.